

30 nM using Lipofectamine RNAiMAX (Invitrogen) in accordance with the manufacturer's instructions. Target sequences of the siRNAs were: occludin (5'-GCAAGACUAUGAGACA-3'), SR-BI (5'-GAGCUUUGGCCUUGGUCUA-3'), CD81 (5'-CUGUGAUGAUGAUCUUCGA-3'), CHC (5'-CUAGCUUUGCACAGUUUAA-3'), Dyn2 (5'-CCCUCAGGAGGCGCUCAA-3'), Cav1 (5'-CCCUAAACACCUCAACGAU-3'), flotillin-1 (5'-CCUAUGACAUCGAGGUCUA-3'), Arf6 (5'-CAGUUCUUGGUAAGUCCU-3'), CtBP1 (5'-GACUCGACGCUGUGCCACA-3') and PAK1 (5'-GCAUCAUUCUGAAGAUU-3'). Target sequences of the siRNAs for claudin-1, PI4K and scrambled negative control were as described previously (Suzuki *et al.*, 2013).

**Immunoblotting.** Cells were washed with PBS and incubated with passive lysis buffer (Promega). Lysates were sonicated for 10 min and added to the same volume of 2 × SDS-PAGE sample buffer. Protein samples were boiled for 10 min, separated by SDS-PAGE and then transferred to PVDF membranes (Merck Millipore). After blocking, membranes were probed with primary antibodies, followed by incubation with peroxidase-conjugated secondary antibody. Antigen-antibody complexes were visualized using an enhanced chemiluminescence detection system (SuperSignal West Pico Chemiluminescent Substrate; Thermo Scientific) in accordance with the manufacturer's protocols.

**Flow cytometry.** Cultured cells detached by treatment with trypsin were incubated with anti-CD81 antibody or anti-mouse IgG antibody for 1 h at 4 °C. After being washed with PBS containing 0.1 % BSA, cells were incubated with an Alexa Fluor 488-conjugated anti-mouse secondary antibody (Invitrogen) for 1 h at 4 °C, washed repeatedly and resuspended in PBS. Analyses were performed using a FACSCalibur system (Becton Dickinson).

**Reagents and antibodies.** Bafilomycin A1 was obtained from Wako Pure Chemical Industries. Alexa Fluor 488-conjugated transferrin was obtained from Invitrogen. For immunoblotting, anti-SR-BI (NB400-104; Novus Biologicals), anti-occludin (71-1500; Invitrogen), anti-claudin-1 (51-9000; Invitrogen), anti-Dyn2 (ab3457; Abcam), anti-Cav1 (N-20; Santa Cruz Biotechnology), anti-flotillin (H-104; Santa Cruz Biotechnology), anti-Arf6 (ab77581; Abcam) and anti-PAK1 (2602; Cell Signaling Technology) rabbit polyclonal antibodies; anti-CD81 (JS-81; BD Biosciences), anti-β-actin (AC-15; Sigma-Aldrich), anti-CHC (23; BD Biosciences), anti-GRAF1 (SAB1400439; Sigma-Aldrich) and anti-glyceraldehyde 3-phosphate dehydrogenase (6C5; Merck Millipore) mouse mAb; and anti-CtBP1 goat polyclonal antibody (C-17; Santa Cruz Biotechnology) were used. For immunofluorescence staining, anti-CHC mAb (X22) and anti-HA rat polyclonal antibody (3F10) were obtained from Thermo Scientific and Roche Applied Science, respectively. Anti-NS5A antibody was a rabbit polyclonal antibody against synthetic peptides. Alexa Fluor 488- or 555-labelled secondary antibodies were obtained from Invitrogen.

**DNA transfection.** Cell monolayers were transfected with plasmid DNA using TransIT-LT1 transfection reagent (Mirus) in accordance with the manufacturer's instructions.

**Treatment of cells with bafilomycin A1 and cell viability.** Cells were preincubated with various concentrations of bafilomycin A1 for 60 min at 37 °C. Preincubated cells were then infected with HCVtcp. Cells treated with 0.1 % DMSO were used as controls. Cell viability was analysed by the Cell Titre-Glo Luminescent Cell Viability Assay (Promega).

**Uptake of transferrin.** Cells were grown on glass coverslips. After cells were transfected with HA-tagged Dyn2 expression plasmids, Alexa Fluor 488-conjugated transferrin at 20 µg ml<sup>-1</sup> was added and incubated for 30 min. Cells were washed with PBS and fixed in 4 % paraformaldehyde.

**Immunofluorescence analysis.** Huh7.5.1 and Huh-7 cells were fixed with 4 % paraformaldehyde in PBS for 30 min, and were then blocked and permeabilized with 0.3 % Triton X-100 in a non-fat milk solution (Block Ace; Snow Brand Milk Products) for 60 min at room temperature. Samples were then incubated with anti-CHC, anti-Dyn2, anti-Cav1, anti-NS5A or anti-HA for 60 min at room temperature, washed three times with PBS, and then incubated with secondary antibodies for 60 min at room temperature. Finally, samples were washed three times with PBS, rinsed briefly in double-distilled H<sub>2</sub>O and mounted with DAPI mounting medium. The signal was analysed using a Leica TCS SPE confocal microscope.

**Luciferase assay.** For quantification of FLuc activity in HCVtcp-infected cells, cells were lysed with passive lysis buffer (Promega) at 72 h post-infection. FLuc activity of the cells was determined using a luciferase assay system (Promega). For quantification of GLuc activity in supernatants of HCVtcp-infected cells, the *Renilla* Luciferase Assay System (Promega) was used. All luciferase assays were performed at least in triplicate.

**Quantification of HCV core protein.** HCV core protein was quantified using a highly sensitive enzyme immunoassay (Lumipulse G1200; Fujirebio) in accordance with the manufacturer's instructions.

## ACKNOWLEDGEMENTS

We are grateful to Francis V. Chisari (Scripps Research Institute) for providing Huh-7 and Huh7.5.1 cells. We would also like to thank M. Sasaki for technical assistance, and T. Kato, A. Murayama and K. Mori for helpful discussion.

## REFERENCES

- Acosta, E. G., Castilla, V. & Damonte, E. B. (2008). Functional entry of dengue virus into *Aedes albopictus* mosquito cells is dependent on clathrin-mediated endocytosis. *J Gen Virol* **89**, 474–484.
- Acosta, E. G., Castilla, V. & Damonte, E. B. (2009). Alternative infectious entry pathways for dengue virus serotypes into mammalian cells. *Cell Microbiol* **11**, 1533–1549.
- Akazawa, D., Date, T., Morikawa, K., Murayama, A., Omi, N., Takahashi, H., Nakamura, N., Ishii, K., Suzuki, T. & other authors (2008). Characterization of infectious hepatitis C virus from liver-derived cell lines. *Biochem Biophys Res Commun* **377**, 747–751.
- Bartosch, B., Vitelli, A., Granier, C., Goujon, C., Dubuisson, J., Pascale, S., Scarselli, E., Cortese, R., Nicosia, A. & Cosset, F. L. (2003). Cell entry of hepatitis C virus requires a set of co-receptors that include the CD81 tetraspanin and the SR-B1 scavenger receptor. *J Bio Chem* **278**, 41624–41630.
- Benedicto, I., Molina-Jimenez, F., Bartosch, B., Cosset, F. L., Lavillette, D., Prieto, J., Moreno-Otero, R., Valenzuela-Fernandez, A., Aldabe, R., Lopez-Cabrera, M. & Majano, P. L. (2009). The tight junction-associated protein occludin is required for a postbinding step in hepatitis C virus entry and infection. *J Virol* **83**, 8012–8020.
- Blanchard, E., Belouzard, S., Goueslain, L., Wakita, T., Dubuisson, J., Wychowski, C. & Rouillé, Y. (2006). Hepatitis C virus entry depends on clathrin-mediated endocytosis. *J Virol* **80**, 6964–6972.
- Blight, K. J., McKeating, J. A. & Rice, C. M. (2002). Highly permissive cell lines for subgenomic and genomic hepatitis C virus RNA replication. *J Virol* **76**, 13001–13014.
- Codran, A., Royer, C., Jaeck, D., Bastien-Valle, M., Baumert, T. F., Kieny, M. P., Pereira, C. A. & Martin, J. P. (2006). Entry of hepatitis C

- virus pseudotypes into primary human hepatocytes by clathrin-dependent endocytosis. *J Gen Virol* 87, 2583–2593.
- Coller, K. E., Berger, K. L., Heaton, N. S., Cooper, J. D., Yoon, R. & Randall, G. (2009). RNA interference and single particle tracking analysis of hepatitis C virus endocytosis. *PLoS Pathog* 5, e1000702.
- Damke, H., Baba, T., van der Bliek, A. M. & Schmid, S. L. (1995). Clathrin-independent pinocytosis is induced in cells overexpressing a temperature-sensitive mutant of dynamin. *J Cell Biol* 131, 69–80.
- Damm, E. M., Pelkmans, L., Kartenbeck, J., Mezzacasa, A., Kurzhalia, T. & Helenius, A. (2005). Clathrin- and caveolin-1-independent endocytosis: entry of simian virus 40 into cells devoid of caveolae. *J Cell Biol* 168, 477–488.
- Evans, M. J., von Hahn, T., Tscherne, D. M., Syder, A. J., Panis, M., Wolk, B., Hatzioannou, T., McKeating, J. A., Bieniasz, P. D. & Rice, C. M. (2007). Claudin-1 is a hepatitis C virus co-receptor required for a late step in entry. *Nature* 446, 801–805.
- Grove, J. & Marsh, M. (2011). The cell biology of receptor-mediated virus entry. *J Cell Biol* 195, 1071–1082.
- Grove, J., Nielsen, S., Zhong, J., Bassendine, M. F., Drummer, H. E., Balfe, P. & McKeating, J. A. (2008). Identification of a residue in hepatitis C virus E2 glycoprotein that determines scavenger receptor BI and CD81 receptor dependency and sensitivity to neutralizing antibodies. *J Virol* 82, 12020–12029.
- Helle, F., Vieyres, G., Elkrief, L., Popescu, C.-I., Wychowski, C., Descamps, V., Castelain, S., Roingeard, P., Duverlie, G. & Dubuisson, J. (2010). Role of N-linked glycans in the functions of hepatitis C virus envelope proteins incorporated into infectious virions. *J Virol* 84, 11905–11915.
- Hoofnagle, J. H. (2002). Course and outcome of hepatitis C. *Hepatology* 36 (Suppl 1), S21–S29.
- Kambara, H., Fukuhara, T., Shiokawa, M., Ono, C., Ohara, Y., Kamitani, W. & Matsuura, Y. (2012). Establishment of a novel permissive cell line for the propagation of hepatitis C virus by expression of microRNA miR122. *J Virol* 86, 1382–1393.
- Kataoka, C., Kaname, Y., Taguwa, S., Abe, T., Fukuhara, T., Tani, H., Moriishi, K. & Matsuura, Y. (2012). Baculovirus GP64-mediated entry into mammalian cells. *J Virol* 86, 2610–2620.
- Kato, N., Mori, K., Abe, K., Dansako, H., Kuroki, M., Ariumi, Y., Wakita, T. & Ikeda, M. (2009). Efficient replication systems for hepatitis C virus using a new human hepatoma cell line. *Virus Res* 146, 41–50.
- Liu, S., Yang, W., Shen, L., Turner, J. R., Coyne, C. B. & Wang, T. (2009). Tight junction proteins claudin-1 and occludin control hepatitis C virus entry and are downregulated during infection to prevent superinfection. *J Virol* 83, 2011–2014.
- Lupberger, J., Zeisel, M. B., Xiao, F., Thumann, C., Fofana, I., Zona, L., Davis, C., Mee, C. J., Turek, M. & other authors (2011). EGFR and EphA2 are host factors for hepatitis C virus entry and possible targets for antiviral therapy. *Nat Med* 17, 589–595.
- Marsh, M. & Helenius, A. (2006). Virus entry: open sesame. *Cell* 124, 729–740.
- Matlin, K. S., Reggio, H., Helenius, A. & Simons, K. (1981). Infectious entry pathway of influenza virus in a canine kidney cell line. *J Cell Biol* 91, 601–613.
- McKeating, J. A., Zhang, L. Q., Logvinoff, C., Flint, M., Zhang, J., Yu, J., Butera, D., Ho, D. D., Dustin, L. B., Rice, C. M. & Balfe, P. (2004). Diverse hepatitis C virus glycoproteins mediate viral infection in a CD81-dependent manner. *Journal of virology* 78, 8496–8505.
- Meertens, L., Bertaux, C. & Dragic, T. (2006). Hepatitis C virus entry requires a critical postinternalization step and delivery to early endosomes via clathrin-coated vesicles. *J Virol* 80, 11571–11578.
- Mercer, J., Schelhaas, M. & Helenius, A. (2010). Virus entry by endocytosis. *Annu Rev Biochem* 79, 803–833.
- Miaczynska, M. & Stenmark, H. (2008). Mechanisms and functions of endocytosis. *J Cell Biol* 180, 7–11.
- Mosso, C., Galván-Mendoza, I. J., Ludert, J. E. & del Angel, R. M. (2008). Endocytic pathway followed by dengue virus to infect the mosquito cell line C6/36 HT. *Virology* 378, 193–199.
- Norkin, L. C., Anderson, H. A., Wolfrom, S. A. & Oppenheim, A. (2002). Caveolar endocytosis of simian virus 40 is followed by brefeldin A-sensitive transport to the endoplasmic reticulum, where the virus disassembles. *J Virol* 76, 5156–5166.
- Pelkmans, L., Kartenbeck, J. & Helenius, A. (2001). Caveolar endocytosis of simian virus 40 reveals a new two-step vesicular-transport pathway to the ER. *Nat Cell Biol* 3, 473–483.
- Pileri, P., Uematsu, Y., Campagnoli, S., Galli, G., Falugi, F., Petracca, R., Weiner, A. J., Houghton, M., Rosa, D., Grandi, G. & Abrignani, S. (1998). Binding of hepatitis C virus to CD81. *Science* 282, 938–941.
- Ploss, A., Evans, M. J., Gaysinskaya, V. A., Panis, M., You, H., de Jong, Y. P. & Rice, C. M. (2009). Human occludin is a hepatitis C virus entry factor required for infection of mouse cells. *Nature* 457, 882–886.
- Sainz, B., Jr, Barretto, N., Martin, D. N., Hiraga, N., Imamura, M., Hussain, S., Marsh, K. A., Yu, X., Chayama, K. & other authors (2012). Identification of the Niemann–Pick C1-like 1 cholesterol absorption receptor as a new hepatitis C virus entry factor. *Nat Med* 18, 281–285.
- Scarselli, E., Ansuini, H., Cerino, R., Roccasecca, R. M., Acali, S., Filocomo, G., Traboni, C., Nicosia, A., Cortese, R. & Vitelli, A. (2002). The human scavenger receptor class B type I is a novel candidate receptor for the hepatitis C virus. *Embo J* 21, 5017–5025.
- Sieczkarski, S. B. & Whittaker, G. R. (2002a). Dissecting virus entry via endocytosis. *J Gen Virol* 83, 1535–1545.
- Sieczkarski, S. B. & Whittaker, G. R. (2002b). Influenza virus can enter and infect cells in the absence of clathrin-mediated endocytosis. *J Virol* 76, 10455–10464.
- Sumpter, R., Jr, Loo, Y.-M., Foy, E., Li, K., Yoneyama, M., Fujita, T., Lemon, S. M. & Gale, M., Jr (2005). Regulating intracellular antiviral defense and permissiveness to hepatitis C virus RNA replication through a cellular RNA helicase, RIG-I. *J Virol* 79, 2689–2699.
- Suzuki, T., Ishii, K., Aizaki, H. & Wakita, T. (2007). Hepatitis C viral life cycle. *Adv Drug Deliv Rev* 59, 1200–1212.
- Suzuki, R., Saito, K., Kato, T., Shirakura, M., Akazawa, D., Ishii, K., Aizaki, H., Kanegae, Y., Matsuura, Y. & other authors (2012). Trans-complemented hepatitis C virus particles as a versatile tool for study of virus assembly and infection. *Virology* 432, 29–38.
- Suzuki, R., Matsuda, M., Watashi, K., Aizaki, H., Matsuura, Y., Wakita, T. & Suzuki, T. (2013). Signal peptidase complex subunit 1 participates in the assembly of hepatitis C virus through an interaction with E2 and NS2. *PLoS Pathog* 9, e1003589.
- Trotard, M., Lepère-Douard, C., Régeard, M., Piquet-Pellorce, C., Lavillette, D., Cosset, F. L., Gripon, P. & Le Seyec, J. (2009). Kinases required in hepatitis C virus entry and replication highlighted by small interference RNA screening. *FASEB J* 23, 3780–3789.
- van der Schaar, H. M., Rust, M. J., Chen, C., van der Ende-Metselaar, H., Wilschut, J., Zhuang, X. & Smit, J. M. (2008). Dissecting the cell entry pathway of dengue virus by single-particle tracking in living cells. *PLoS Pathog* 4, e1000244.
- Vieyres, G., Thomas, X., Descamps, V., Duverlie, G., Patel, A. H. & Dubuisson, J. (2010). Characterization of the envelope glycoproteins associated with infectious hepatitis C virus. *J Virol* 84, 10159–10168.
- Zhong, J., Gastaminza, P., Cheng, G., Kapadia, S., Kato, T., Burton, D. R., Wieland, S. F., Uprichard, S. L., Wakita, T. & Chisari, F. V. (2005). Robust hepatitis C virus infection *in vitro*. *Proc Natl Acad Sci U S A* 102, 9294–9299.

# Hepatology Journal

Copy of e-mail Notification

Your article (HEP-13-2458.R1.27197) from Hepatology is available for download.

Dear Author,

Your article page proofs for Hepatology are ready for review. John Wiley & Sons has made this article available to you online for faster, more efficient editing. Please follow the instructions below and you will be able to access a PDF version of your article as well as relevant accompanying paperwork.

First, make sure you have a copy of Adobe Acrobat Reader software to read these files. This is free software and is available for user downloading at <http://www.adobe.com/products/acrobat/readstep.html>.

Open your web browser, and enter the following web address:

<http://115.111.50.156/jw/retrieval.aspx>

You will be prompted to log in, and asked for a password. Your login name will be your email address, and your password will be 14c0826f28d8

Example:

Login: your e-mail address

Password: 14c0826f28d8

The site contains one file, containing:

- Author Instructions Checklist
- Adobe Acrobat Users - NOTES tool sheet
- Reprint Order Information
- A copy of your page proofs for your article

Read your page proofs carefully and:

- indicate changes or corrections in the margin of the page proofs or via Adobe Notes
- answer all queries (footnotes A,B,C, etc.) on the last page of the PDF proof
- proofread any tables and equations carefully
- check your figure legends for accuracy

Within 48 hours, please return via e-mail or fax all materials to the address given below. This will include:

Page proofs with corrections

Return to:

Hepatology Production

# Hepatology Journal

Copy of e-mail Notification

E-mail: [hepjournal@wiley.com](mailto:hepjournal@wiley.com)

John Wiley & Sons, Inc.

111 River Street, Mail Stop 8-02

Hoboken, NJ 07030

TEL: (201) 748-5762

Technical problems? If you experience technical problems downloading your file or any other problem with the website listed above, please contact Balaji/Sam (e-mail: [wileycs@kwglobal.com](mailto:wileycs@kwglobal.com)).

Questions regarding your article? Please don't hesitate to contact me with any questions about the article itself, or if you have trouble interpreting any of the questions listed at the end of your file. **REMEMBER TO INCLUDE YOUR ARTICLE NO. (HEP-13-2458.27197) WITH ALL CORRESPONDENCE.** This will help both of us address your query most efficiently.

As this e-proofing system was designed to make the publishing process easier for everyone, we welcome any and all feedback. Thanks for participating in our e-proofing system!

This e-proof is to be used only for the purpose of returning corrections to the publisher.

Sincerely,

Joyce Griffin Production Editor

Hepatology Production, Global Research, John Wiley & Sons

E-mail: [hepjournal@wiley.com](mailto:hepjournal@wiley.com)



111 RIVER STREET, HOBOKEN, NJ 07030

## HEPATOLOGY PRODUCTION

**\*\*\*IMMEDIATE RESPONSE REQUIRED\*\*\***

Please follow these instructions to avoid delay of publication.

**READ PROOFS CAREFULLY**

- This will be your only chance to review these proofs. **Please note that once your corrected article is posted online, it is considered legally published, and cannot be removed from the Web site for further corrections.**
- Please note that the volume and page numbers shown on the proofs are for position only.

**ANSWER ALL QUERIES ON PROOFS** (Queries for you to answer are attached as the last page of your proof.)

- Mark all corrections directly on the proofs. Note that excessive author alterations may ultimately result in delay of publication and extra costs may be charged to you.

**CHECK FIGURES AND TABLES CAREFULLY**

- Check size, numbering, and orientation of figures.
- All images in the PDF are downsampled (reduced to lower resolution and file size) to facilitate Internet delivery. These images will appear at higher resolution and sharpness in the printed article.
- Review figure legends to ensure that they are complete.
- Check all tables. Review layout, title, and footnotes.

RETURN  PROOFS

**PLEASE RETURN PROOFS (VIA FAX, E-MAIL, OR OVERNIGHT COURIER) WITHIN 48 HOURS OF RECEIPT TO:**

QUESTIONS?

**Joyce Griffin, Production Editor  
Hepatology Production  
E-mail: [hepjournal@wiley.com](mailto:hepjournal@wiley.com)  
FAX: 201-748-6281/6182**

John Wiley & Sons, Inc.  
111 River St., Mail Stop 8-02  
Hoboken, NJ 07030  
Phone: 201-748-5762

Refer to journal acronym and article production number  
(i.e., HEP 00-0001.20000 for HEPATOLOGY ms 00-0001.20000).

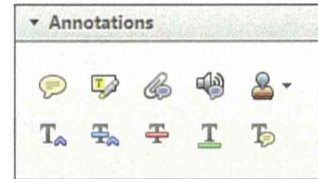
USING e-ANNOTATION TOOLS FOR ELECTRONIC PROOF CORRECTION

Required software to e-Annotate PDFs: **Adobe Acrobat Professional** or **Adobe Reader** (version 8.0 or above). (Note that this document uses screenshots from **Adobe Reader X**)  
 The latest version of Acrobat Reader can be downloaded for free at: <http://get.adobe.com/reader/>

Once you have Acrobat Reader open on your computer, click on the **Comment** tab at the right of the toolbar:



This will open up a panel down the right side of the document. The majority of tools you will use for annotating your proof will be in the **Annotations** section, pictured opposite. We've picked out some of these tools below:



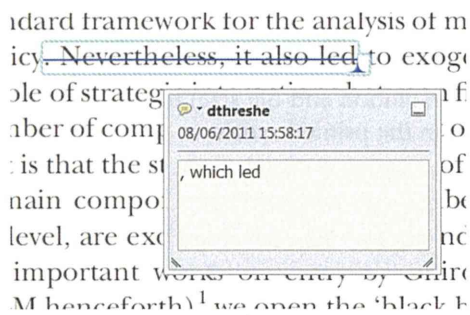
**1. Replace (Ins) Tool – for replacing text.**



Strikes a line through text and opens up a text box where replacement text can be entered.

**How to use it**

- Highlight a word or sentence.
- Click on the **Replace (Ins)** icon in the Annotations section.
- Type the replacement text into the blue box that appears.



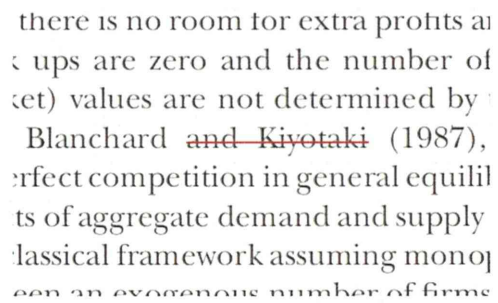
**2. Strikethrough (Del) Tool – for deleting text.**



Strikes a red line through text that is to be deleted.

**How to use it**

- Highlight a word or sentence.
- Click on the **Strikethrough (Del)** icon in the Annotations section.



**3. Add note to text Tool – for highlighting a section to be changed to bold or italic.**

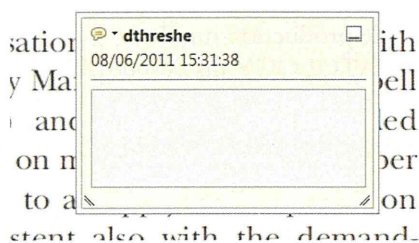


Highlights text in yellow and opens up a text box where comments can be entered.

**How to use it**

- Highlight the relevant section of text.
- Click on the **Add note to text** icon in the Annotations section.
- Type instruction on what should be changed regarding the text into the yellow box that appears.

dynamic responses of mark ups  
 ent with the **VAR** evidence



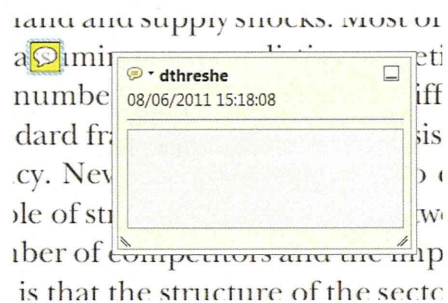
**4. Add sticky note Tool – for making notes at specific points in the text.**



Marks a point in the proof where a comment needs to be highlighted.


**How to use it**

- Click on the **Add sticky note** icon in the Annotations section.
- Click at the point in the proof where the comment should be inserted.
- Type the comment into the yellow box that appears.



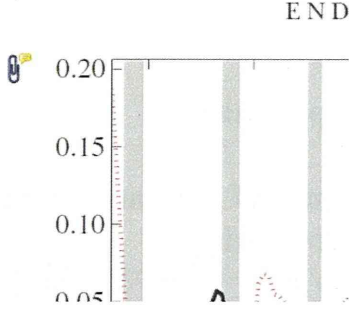
USING e-ANNOTATION TOOLS FOR ELECTRONIC PROOF CORRECTION

**5. Attach File Tool – for inserting large amounts of text or replacement figures.**


 Inserts an icon linking to the attached file in the appropriate place in the text.

**How to use it**

- Click on the **Attach File** icon in the Annotations section.
- Click on the proof to where you'd like the attached file to be linked.
- Select the file to be attached from your computer or network.
- Select the colour and type of icon that will appear in the proof. Click OK.




**6. Add stamp Tool – for approving a proof if no corrections are required.**

 Inserts a selected stamp onto an appropriate place in the proof.

**How to use it**

- Click on the **Add stamp** icon in the Annotations section.
- Select the stamp you want to use. (The **Approved** stamp is usually available directly in the menu that appears).
- Click on the proof where you'd like the stamp to appear. (Where a proof is to be approved as it is, this would normally be on the first page).

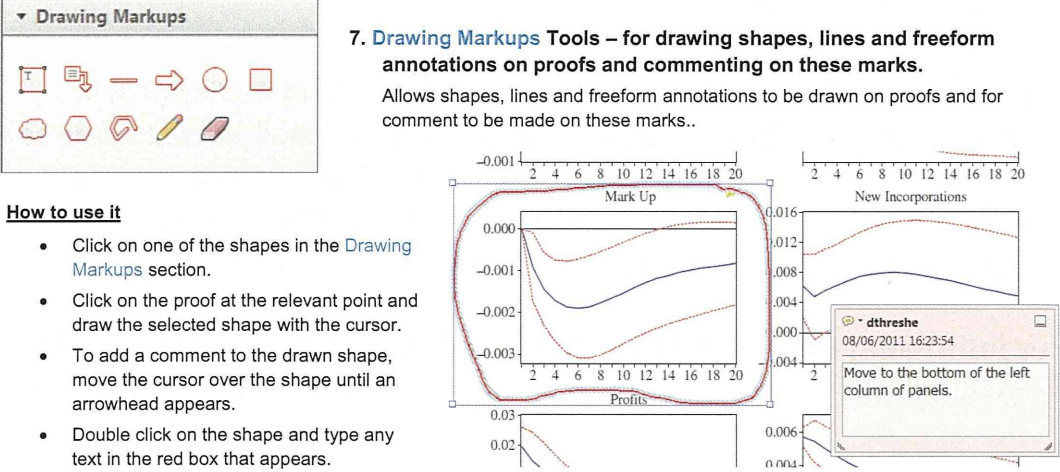


**7. Drawing Markups Tools – for drawing shapes, lines and freeform annotations on proofs and commenting on these marks.**

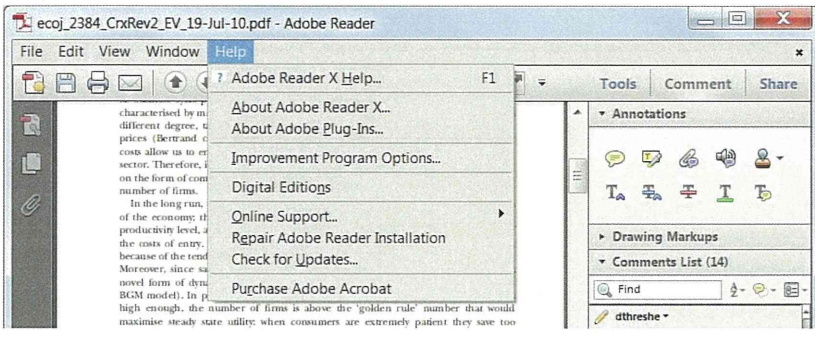
Allows shapes, lines and freeform annotations to be drawn on proofs and for comment to be made on these marks..

**How to use it**

- Click on one of the shapes in the **Drawing Markups** section.
- Click on the proof at the relevant point and draw the selected shape with the cursor.
- To add a comment to the drawn shape, move the cursor over the shape until an arrowhead appears.
- Double click on the shape and type any text in the red box that appears.



For further information on how to annotate proofs, click on the **Help** menu to reveal a list of further options:





### **Additional reprint purchases**

Should you wish to purchase additional copies of your article, please click on the link and follow the instructions provided:

<https://caesar.sheridan.com/reprints/redirect.php?pub=10089&acro=HEP>

Corresponding authors are invited to inform their co-authors of the reprint options available.

Please note that regardless of the form in which they are acquired, reprints should not be resold, nor further disseminated in electronic form, nor deployed in part or in whole in any marketing, promotional or educational contexts without authorization from Wiley. Permissions requests should be directed to mail to: [permissionsus@wiley.com](mailto:permissionsus@wiley.com)

For information about 'Pay-Per-View and Article Select' click on the following link: [wileyonlinelibrary.com/aboutus/ppv-articleselect.html](http://wileyonlinelibrary.com/aboutus/ppv-articleselect.html)



# Development of Hepatitis C Virus Genotype 3a Cell Culture System

AQ1

Sulyi Kim,<sup>1</sup> Tomoko Date,<sup>1</sup> Hiroshi Yokokawa,<sup>1,2</sup> Tamaki Kono,<sup>1</sup> Hideki Aizaki,<sup>1</sup> Patrick Maurel,<sup>1,3</sup> Claire Gondeau,<sup>3,4</sup> and Takaji Wakita<sup>1</sup>

Hepatitis C virus (HCV) genotype 3a infection poses a serious health problem worldwide. A significant association has been reported between HCV genotype 3a infections and hepatic steatosis. Nevertheless, virological characterization of genotype 3a HCV is delayed due to the lack of appropriate virus cell culture systems. In the present study we established the first infectious genotype 3a HCV system by introducing adaptive mutations into the S310 strain. HCV core proteins had different locations in JFH-1 and S310 virus-infected cells. Furthermore, the lipid content in S310 virus-infected cells was higher than Huh7.5.1 cells and JFH-1 virus-infected cells as determined by the lipid droplet staining area. **Conclusion:** We believe that this genotype 3a infectious cell culture system will be a useful experimental model for studying genotype 3a viral life cycles, molecular mechanisms of pathogenesis, and genotype 3a-specific antiviral drug development. (HEPATOLOGY 2014;00:000-000)

About 170 million people worldwide are infected with hepatitis C virus (HCV), which causes chronic liver disease at a high rate, leading to complications including endstage liver disease, liver cirrhosis, and hepatocellular carcinoma.<sup>1</sup> HCV is classified into seven major genotypes.<sup>2</sup> Genotype 1b is the most prevalent HCV genotype in Asian countries, followed by genotype 3a. Genotype 3a infections are more prevalent in South Asian countries with large populations.<sup>3,4</sup> A high incidence of hepatic steatosis is associated with genotype 3a infection.<sup>5-7</sup> Interferon and ribavirin combination therapy is not satisfactory in genotype 3a-infected patients, although it is more effective than in genotype 1b-infected patients.<sup>5</sup> The recently developed protease inhibitors telaprevir and boceprevir are also less effective against genotype 3a infection.<sup>8</sup> New antiviral drug development against genotype 3a HCV is necessary to improve treatment efficiency in genotype 3a-infected patients.

HCV subgenomic replicon systems are useful tools for the study of viral replication mechanisms and anti-

viral drug development. Recently, genotype 3a replicon systems were established.<sup>9,10</sup> The S310 replicon with adaptive mutations replicated efficiently in cell culture. Genotype 3a infections have a different pathogenesis as compared to other genotype infections (for example, steatosis). Previous studies demonstrated that cells expressing genotype 3a core protein had increased lipid accumulation.<sup>11-13</sup> Therefore, an efficient infectious viral system recapitulating the full life cycle is now essential to determine the precise pathogenesis of genotype 3a infection.

In the present study we established an infectious genotype 3a HCV cell culture system by using S310 strains. The full-length S310 clones replicated efficiently and produced infectious viral particles. There were different HCV core localization patterns between genotype 3a S310- and genotype 2a JFH-1-infected cells. Interestingly, the lipid content in S310 virus-infected cells was higher than Huh7.5.1 cells and JFH-1 virus-infected cells as determined by lipid droplet staining area. This cell culture system will be very

*Abbreviations:* DMEM, Dulbecco's Modified Eagle Medium; HCV, hepatitis C virus; IgG, immunoglobulin G; LD, lipid droplet; MOI, multiplicity of infection; RT-PCR, reverse-transcriptase polymerase chain reaction; SGR, subgenomic replicon.

From the <sup>1</sup>Department of Virology II, National Institute of Infectious Diseases, Tokyo, Japan; <sup>2</sup>Pharmaceutical Research Laboratories, Toray Industries, Inc., Kanagawa, Japan; <sup>3</sup>Inserm U1040, Biotherapy Research Institute, Montpellier, France; <sup>4</sup>Department of Hepato-gastroenterology A, Hospital Saint Eloi, CHU Montpellier, France.

Received November 28, 2013; accepted April 29, 2014.

Supported by Grants-in-Aid for Scientific Research from the Japan Society for the Promotion of Science, from the Ministry of Health, Labour and Welfare of Japan, from the Ministry of Education, Culture, Sports, Science and Technology of Japan, and from the Research on Health Sciences Focusing on Drug Innovation from the Japan Health Sciences Foundation.

useful for the study of viral life cycles, molecular mechanisms of pathogenesis, and specific antiviral drug development for genotype 3a HCV.

## Materials and Methods

Details of the procedures are described in the Supporting Information.

**Cell Culture.** HuH-7 cells (obtained from Dr. Francis V. Chisari, Scripps Research Institute California) and a derivative cell line, Huh7.5.1 cells (obtained from Dr. Francis V. Chisari) were cultured as described in the Supporting Information.

**HCV Plasmid Construction.** Plasmids used in the analysis were constructed based on pS310 (S310/A, DDBJ/EMBL/GenBank accession number: AB691595).<sup>9</sup> We constructed the full-length adapted pS310 by introducing the adaptive mutations from the SGR-S310 replicon assay. pJ6/JFH1 was previously obtained from pJFH1 by replacement with the 5' untranslated region (UTR) to p7 region (EcoRI-BclI) of the J6CF strain (a kind gift from Dr. Jens Bukh).<sup>14</sup> pS310/JFH1 was obtained from pJFH1 by replacement with the core to NS2 C3 junction of the pS310 strain.<sup>15</sup> pS310/JFH1 thus included nucleotide (nt) 1 to 2892 (amino acid [aa] 1 to 851) of S310 and nt 2888 to 9678 (aa 850 to 3033) of JFH-1 (accession number: AB047639).

**RNA Synthesis and Transfection.** Full-length HCV RNA was synthesized from pS310, pJFH1, pJ6/JFH1, pS310/JFH1 and the derivatives of pS310 constructs with adaptive mutations. The synthesized HCV RNA (10  $\mu$ g) was transfected into Huh7.5.1 cells by electroporation, as described previously.<sup>16-18</sup>

**Quantification of HCV Core Protein and RNA.** The concentrations of HCV core protein in the culture media and cell lysates were measured by a chemiluminescent enzyme immunoassay (Lumipulse II HCV core assay, Ortho Clinical Diagnostics, Tokyo, Japan).<sup>19</sup> Real-time quantitative reverse-transcription polymerase chain reaction (RT-PCR) was performed to determine the copy numbers of HCV RNA as described previously.<sup>20</sup>

**RT-PCR and Sequencing Analysis.** Total RNA was extracted and purified from the culture medium or cell pellet of the HCV RNA-transfected cells. HCV

cDNA was synthesized and amplified by RT-PCR as described previously.<sup>21-23</sup> The sequence of each amplified DNA was determined directly by using specific primers.

**Determination of Infectivity.** Infectivity of HCV was quantified by counting the infected foci by using fluorescence microscopy (Olympus, Tokyo, Japan), and the infectivity was expressed as the number of focus-forming units per milliliter (ffu/mL).<sup>16,24</sup>

**Immunofluorescence Analysis and Lipid Content Quantification.** Transfected or infected cells were fixed and then stained with anti-core monoclonal antibody (2H9), DAPI, and BODIPY to determine the sublocalization of core protein, nucleus, and lipid droplets (LDs), respectively. BioZero (Keyence, Tokyo, Japan) or Leica TSE SPE confocal fluorescence microscopy (Leica Microsystems, Wetzlar, Germany) were used for the observation. The LD content of cells was quantified by MetaMorph (Leica MM AF Software) analysis.<sup>25</sup>

**Western Blot Analysis.** Cell lysates were separated by sodium dodecyl sulfate-polyacrylamide gel electrophoresis (SDS-PAGE) and transferred to a PVDF membrane. HCV proteins (core, E2, and NS3) and host proteins were detected by specific antibodies.

**Sucrose Density Gradient Analysis.** Culture medium derived from the transfected cells was analyzed by sucrose gradient ultracentrifugation analysis.

**Anti-HCV Drug Treatment.** HCV-infected cells were tested with various concentrations of interferon  $\alpha$  (IFN $\alpha$ , MSD K.K., Tokyo, Japan), the NS3 protease inhibitor VX-950 (Selleck Chemicals, Houston, TX), the NS5A inhibitor BMS-790052 (Selleck Chemicals), an immunosuppressant cyclosporin A (CsA, Sigma, St. Louis, MO) or the NS5B polymerase inhibitors JTK-109 (Japan Tobacco, Osaka, Japan) and PSI-6130 (Pharmasset, Princeton, NJ). After a 72-hour incubation the culture media were harvested and HCV core protein levels were quantified.

**Statistical Analysis.** Results were obtained from at least three independent experiments. Data are expressed as the mean  $\pm$  SD. Statistical analysis was performed using Welch's t-test.  $P < 0.05$  was considered statistically significant.

Address reprint requests to: Takaji Wakita, M.D., Ph.D., Department of Virology II, National Institute of Infectious Diseases, 1-23-1 Toyama, Shinjuku, Tokyo 162-8640, Japan. E-mail: wakita@nih.go.jp; fax: +81-3-5285-1161.

Copyright © 2014 by the American Association for the Study of Liver Diseases.

View this article online at wileyonlinelibrary.com.

DOI 10.1002/hep.27197

Potential conflict of interest: Nothing to report.

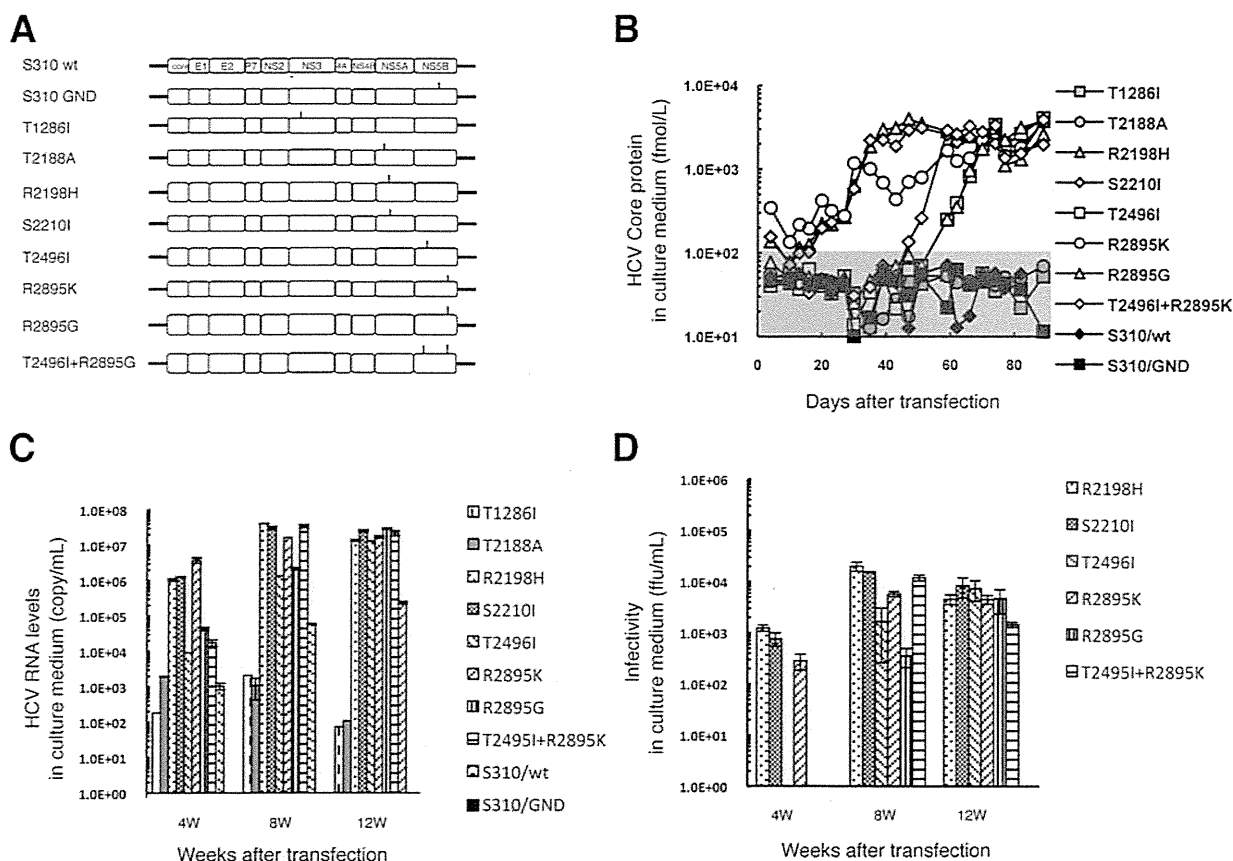


Fig. 1. Structure of full-length adapted S310 constructs and long-term culture of full-length adapted S310 clones. (A) Each mutation from subgenomic replicon clones was introduced into full-length wild-type S310. The position of each mutation is indicated by vertical lines. (B) Huh7.5.1 cells were transfected with the transcribed RNA from each construct. The cells were passaged every 3-5 days and HCV core protein levels in the culture medium at each passage were determined. Gray zone ( $<100$  fmol/L) indicates the value below the detection limit, which was determined by mean  $\pm 3$  SD of the detection values of control culture media. (C) RNAs in the culture medium were isolated. Copy numbers of HCV RNA were determined by real-time detection RT-PCR. The culture medium at 4, 8, and 12 weeks after transfection was used. (D) Infectious titers in the culture medium were determined by focus formation assay. (E) Each passaged cell was seeded onto a slide glass. The cells were fixed, probed with the core specific antibody (green) or DAPI for nucleus staining (blue), and examined by confocal microscopy. The cells at 4, 8, and 12 weeks after transfection are shown. (F) Western blot analysis. Cell lysates were prepared from S310 clones (1; R2198H, 2; S2210I, 3; T2496I, 4; R2895K, 5; R2895G, 6; T2496I+R2895K), Huh7.5.1 cells (7), JFH-1-infected cells (8), and J6/JFH1-infected cells (9). Protein (20  $\mu$ g) was separated by 12.5% SDS-PAGE, and each protein was detected by core, E2, NS3, beta actin, and GAPDH antibody. Arrows indicate the position of each protein. All assays were performed in triplicate, and data are presented as means  $\pm$  standard deviation.

## Results

**Full-Length Constructs With Adaptive Mutations.** In our previous study, several adaptive mutations were found in the genotype 3a S310 subgenomic replicon assay.<sup>9</sup> Those mutations were T1286I (NS3), T2188A (NS5A), R2198H (NS5A), S2210I (NS5A), T2496I (NS5B), R2895K (NS5B), R2895G (NS5B), and T2496I (NS5B) + R2895G (NS5B). We introduced these mutations into full-length S310 wild-type constructs (Fig. 1A).

**Full-Length HCV Replication and Viral Production in Long-Term Culture.** Viral RNA was synthesized from the full-length S310 wild- and mutant-type constructs and transfected into Huh7.5.1 cells. To examine whether these S310 constructs with adaptive

mutations could continuously produce infectious virus, transfected cells were serially passaged and secreted HCV core protein levels in the culture medium were monitored (Fig. 1B). After RNA transfection, the HCV core protein levels of three mutant-type S310 constructs (R2198H, S2210I, and R2895K) continuously increased, and finally they plateaued at  $\sim 2,000$ - $4,000$  fmol/L. Interestingly, from 6-8 weeks after transfection the HCV core protein levels of the other three clones with different adaptive mutations (T2496I, R2895G, and T2496I + R2896K) increased rapidly, and their core protein levels also reached the same levels as the former three clones (R2198H, R2210I, and R2895K). Two other mutant-type (T1286I, T2188A) and wild-type S310 constructs as well as replication-incompetent mutant S310/GND

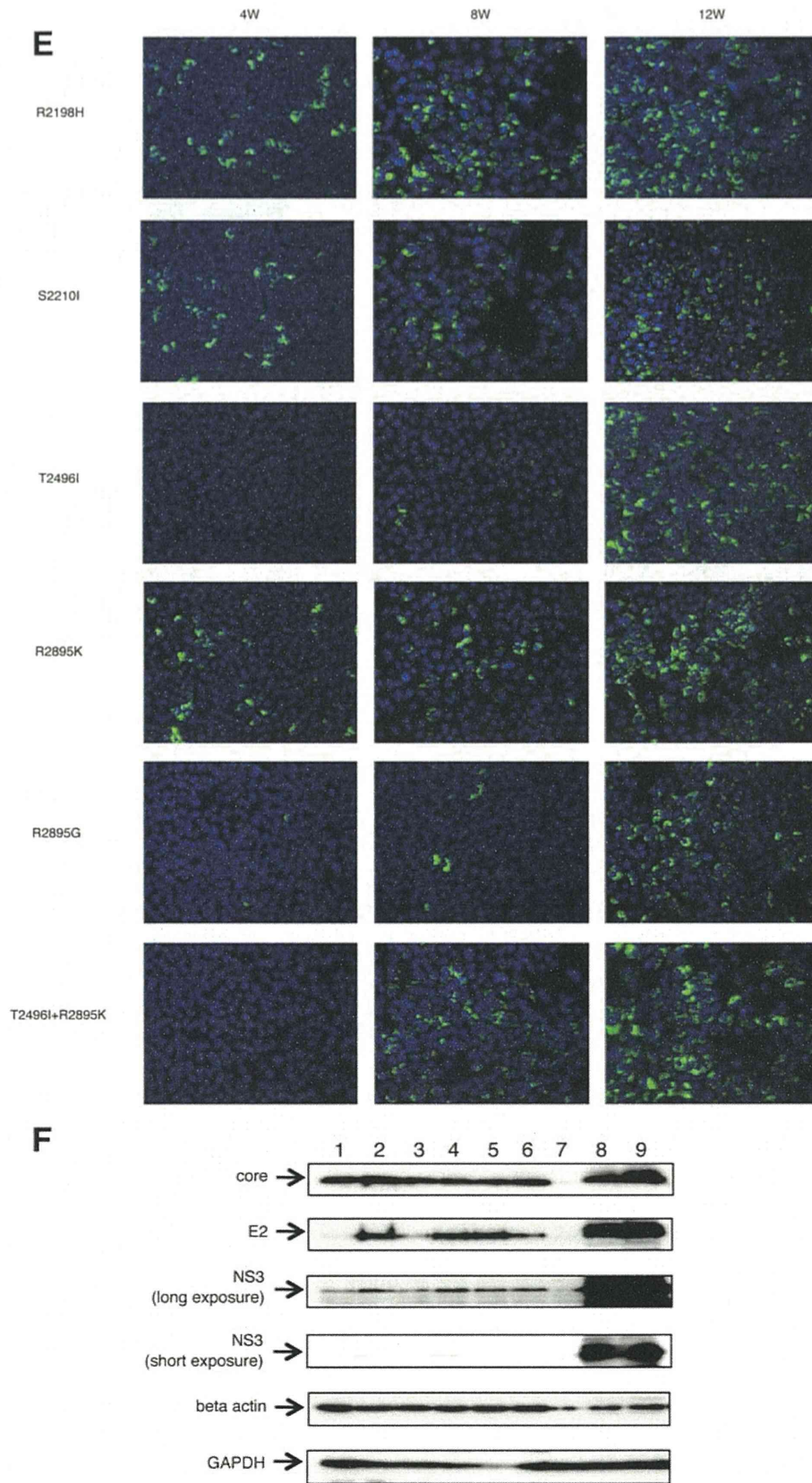


Fig. 1. (Continued)

C  
O  
L  
O  
R

did not secrete any HCV core protein during the observation period. We also determined the HCV RNA levels and infectivity in the culture medium at 4, 8, and 12 weeks after transfection (Fig. 1C,D). The three clones with adaptive mutations (R2198H, R2210I, and R2895K) had higher HCV RNA levels and infectivity than the other clones at 4 weeks after transfection, and their levels increased at 8 and 12 weeks after transfection. The other three clones (T2496I, R2895G, and T2496I + R2896K) had lower levels of HCV RNA and infectivity at 4 weeks after transfection, but from 8 weeks after transfection their levels were similar to the levels of the former three clones. To analyze the mechanism of this discrepancy, we determined the sequences of culture medium of six

T1 S310 clones 82 days after transfection (D82) (Table 1). Interestingly, two clones (S2210I and R2895K) that started to secrete infectious virus at earlier timepoints did not have amino acid mutations. R2198H also started to secrete infectious virus at earlier timepoints, although the virus genome had mutations in the E2 and NS3 regions (Table 1). These mutations may be necessary to produce infectious virus in this clone, but we found different mutations in the R2198H virus in an independent repeated experiment (data not shown). The virus genomes of the three other clones (T2496I, R2895G, and T2496I + R2896K) had several mutations in the E2, NS3, NS4B, NS5a, or NS5B regions (Table 1).

To examine whether the replicating virus in the transfected cells could spread to the surrounding cells, the passaged transfected cells were immunostained with anti-core monoclonal antibody (Fig. 1E). We found a greater number of positive cells in three of the clones (R2198H, R2210I, and R2895K), even at 4 weeks after transfection, compared to the others, and the numbers of positive cells increased at 8 and 12 weeks after transfection. On the other hand, the other three clones (T2496I, R2895G, and T2496I + R2896K) began to get more infected at a later timepoint (8 weeks after transfection), and they showed similar numbers of positive cells at 12 weeks after transfection.

Viral protein expression in the S310-transfected cells was detected by western blotting (Fig. 1F). The core protein expression levels were similar in S310 RNA-transfected cells as compared with JFH-1 and J6/JFH1. However, E2 and NS3 protein expression levels were lower than for JFH-1 and J6/JFH1, probably due to the lower affinity of these antibodies to genotype 3a virus. We failed to detect any other NS proteins with the available antibodies. Interestingly, lower E2 protein expression levels were found in lanes 1, 3, and 6 than

**Table 1. Sequence Analysis and Neutralization With AP33 Antibody of Culture Medium of 82 Days After Transfection**

S310 Clone	Amino Acid Mutations	Regions	AP33 IC <sub>50</sub> (μg/mL)
R2198H	T416A	E2	0.0514
	H579R	E2	
	A1071V	NS3	
	K1412Q	NS3	
	H1967N	NS4B	
S2210I	ND	-	0.0472
T2496I	T416S	E2	0.0642
	A1071V	NS3	
	D1281N	NS3	
	V1756L	NS4B	
	R2895K	NS5B	
R2895K	ND	-	0.0747
R2895G	I1817V	NS4B	0.0615
	G2895A	NS5B	
	T2999S	NS5B	
T2496I + R2985K	T416N	E2	0.0413
	G2326A	NS5A	
	S2357L	NS5A	
	C2429R	NS5A	

ND, not detected.

in the other lanes, although there were no such differences in core protein expression levels. By the sequencing analysis of the virus genome, R2198H, T2496I, and T2496I + R2895K, which had the weaker E2 signals in western blotting, each had a nonsynonymous substitution at amino acid position 416 (R2198H; T to A, T2496I; T to S, T2496I+R2895G; T to N, respectively). This position is located in the epitope of AP33, the anti-E2 antibody. The other three clones (S2210I, R2895K, and R2895G) did not have mutations in the E2 region. Therefore, it appeared that the E2 mutations might disturb antibody binding to E2 protein. To confirm whether neutralization of AP33 was affected by T416 mutations, we determined the 50% inhibitory concentrations (IC<sub>50</sub>) of AP33 neutralization for each mutant virus clone. However, all clones had similar IC<sub>50</sub> values (Table 1). Thus, mutations in the anti-E2 antibody epitope region influenced the results of the western blotting assay but not the neutralization assay.

To examine the viral replication and production levels at the late stage of the long-term culture, the HCV core protein levels, RNA levels, and infectivity of the cell culture medium collected 82 days after transfection were determined (Table 2). HCV core protein levels, RNA levels, and infectivity of the six S310 clones were at approximately one-tenth of the levels of the JFH-1 wild-type virus. However, these levels of infectivity (~1,000-6,000 ffu/mL) might be sufficient to maintain secreted S310 virus production

T2

**Table 2. Quantification of HCV Core Protein Level, RNA Level, and Infectivity of Culture Medium of 82 Days After Transfection**

Mutations	Core (fmol/L)	RNA (copy/ml)	Infectivity (ffu/ml)
R2198H	2,652	1.80E+07	1,000
S2210I	3,334	8.80E+07	4,167
T2496I	3,496	4.33 E+07	2,708
R2895K	4,716	7.83 E+07	6,042
R2895G	1,763	4.11 E+07	417
T2496I+R2895K	2,728	6.26 E+07	1,806
JFH-1	20,932	3.34 E+08	34,722
J6/JFH1	83,388	2.08 E+08	72,917

and replication, since S310 clones could continuously produce the infectious virus in long-term culture (Fig. 1).

**Characterization of Cell Culture-Adapted S310 Virus.** To characterize the secreted infectious viral particles, we analyzed the culture medium of four S310 clones (R2198H, S2210I, R2895K, and T2496I+ R2895K) by sucrose density gradient centrifugation. HCV particles produced in cell culture with the S310 clones showed major peaks of HCV core protein, RNA, and infectivity at 1.15 mg/mL F2 (Fig. 2). JFH-1 also exhibited similar profiles of HCV

core proteins and RNA, but the peak infectivity titers were usually located in a lighter fraction.<sup>18,26</sup> The locations of the peak infectivity titers of S310 clones were different from JFH-1.

S310 viruses (D82), JFH-1 wild-type virus, and J6/JFH1 virus were inoculated into Huh7.5.1 cells at a multiplicity of infection (MOI) of 0.3. To determine whether the cells were successfully infected, we determined and compared the intracellular and extracellular core protein levels of S310 viruses with JFH-1 and J6/JFH1 virus at 24, 48, and 72 hours after infection. Both the intracellular and extracellular core protein levels of all S310 viruses were similar to the levels of JFH-1 wild-type virus, but lower than the levels of J6/JFH1 chimeric virus (Fig. 3A,B). We also evaluated HCV RNA levels and obtained similar results with HCV core protein levels (data not shown).

Next, we determined the neutralization of the infection of these viruses by using anti-CD81 antibody (JS81). Anti-CD81 antibody treatment inhibited the infection of Huh7.5.1 cells by ~99% as compared to control IgG (Fig. 3C,D). S310 virus infection was also inhibited by AP33 anti-E2 antibody (Table 1). It is thus suggested that the S310 viruses utilize similar

F3

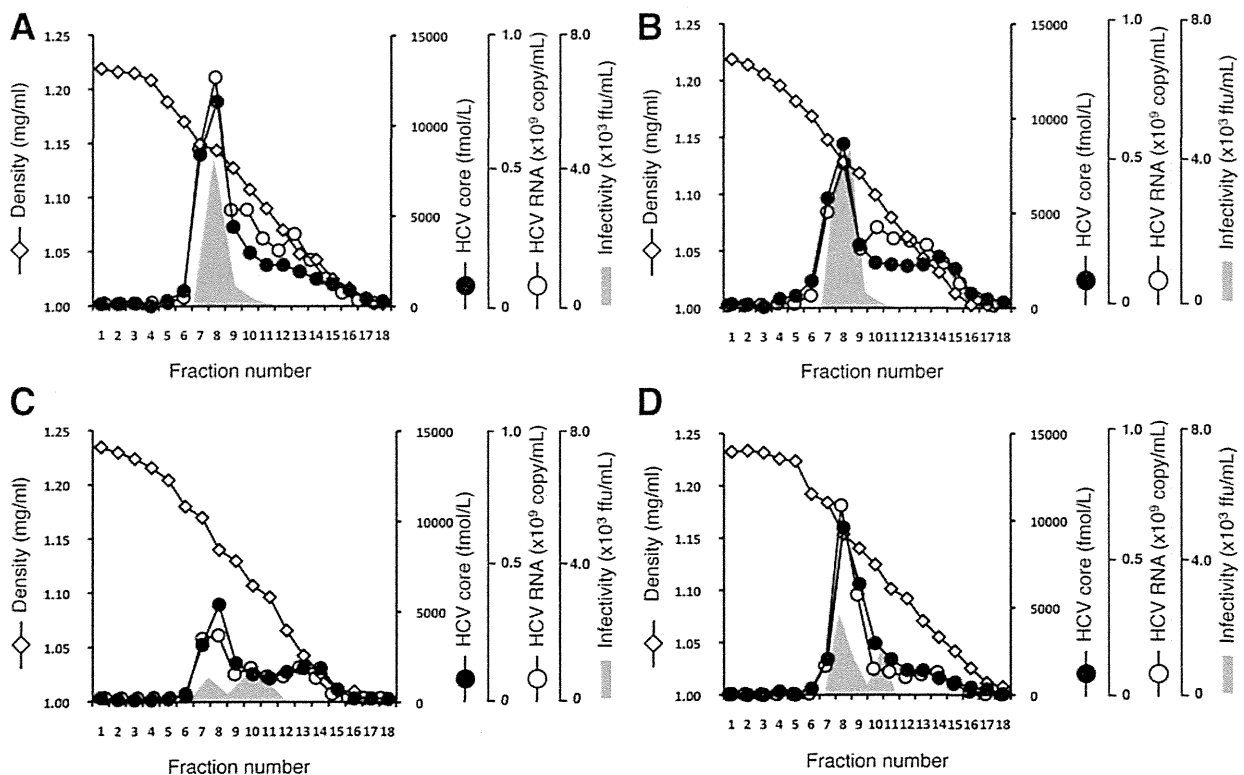


Fig. 2. Sucrose density gradient analysis of the culture medium at 8 weeks after transfection. (A) R2198H, (B) S2210I, (C) R2895K, (D) T2496I+R2895K. Culture medium was overlaid on the stepwise sucrose density gradient (0%, 10%, 20%, 30%, 40%, 50%, and 60% sucrose) and centrifuged for 18 hours at 35,000g at 4°C. A total of 18 fractions were collected from the bottom of the tubes, and density, HCV core protein level, HCV RNA level, and infectivity in each fraction were determined.

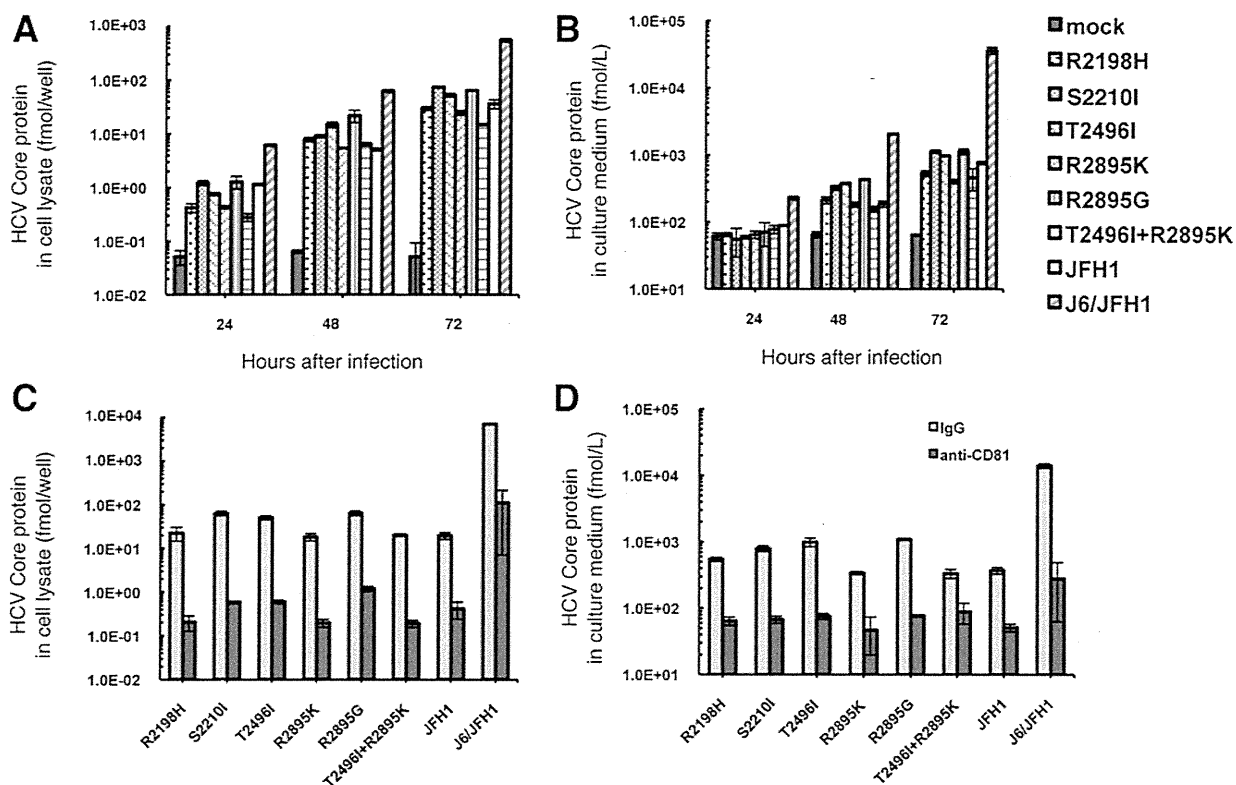


Fig. 3. Comparative analysis with the S310 viruses, JFH-1 and J6/JFH1. (A), (B) Huh7.5.1 cells were infected with the S310 viruses, JFH-1 and J6/JFH1, at an MOI of 0.3. HCV core protein levels in the cell lysate (A) and culture medium (B) were measured at 24, 48, and 72 hours after infection. (C,D) Infection with the adapted S310, JFH-1, and J6/JFH1 virus particles was inhibited by adding anti-CD81 antibody. IgG: normal human immunoglobulin G, anti-CD81: monoclonal anti-CD81 antibody. All assays were performed in triplicate, and data are presented as means  $\pm$  standard deviation.

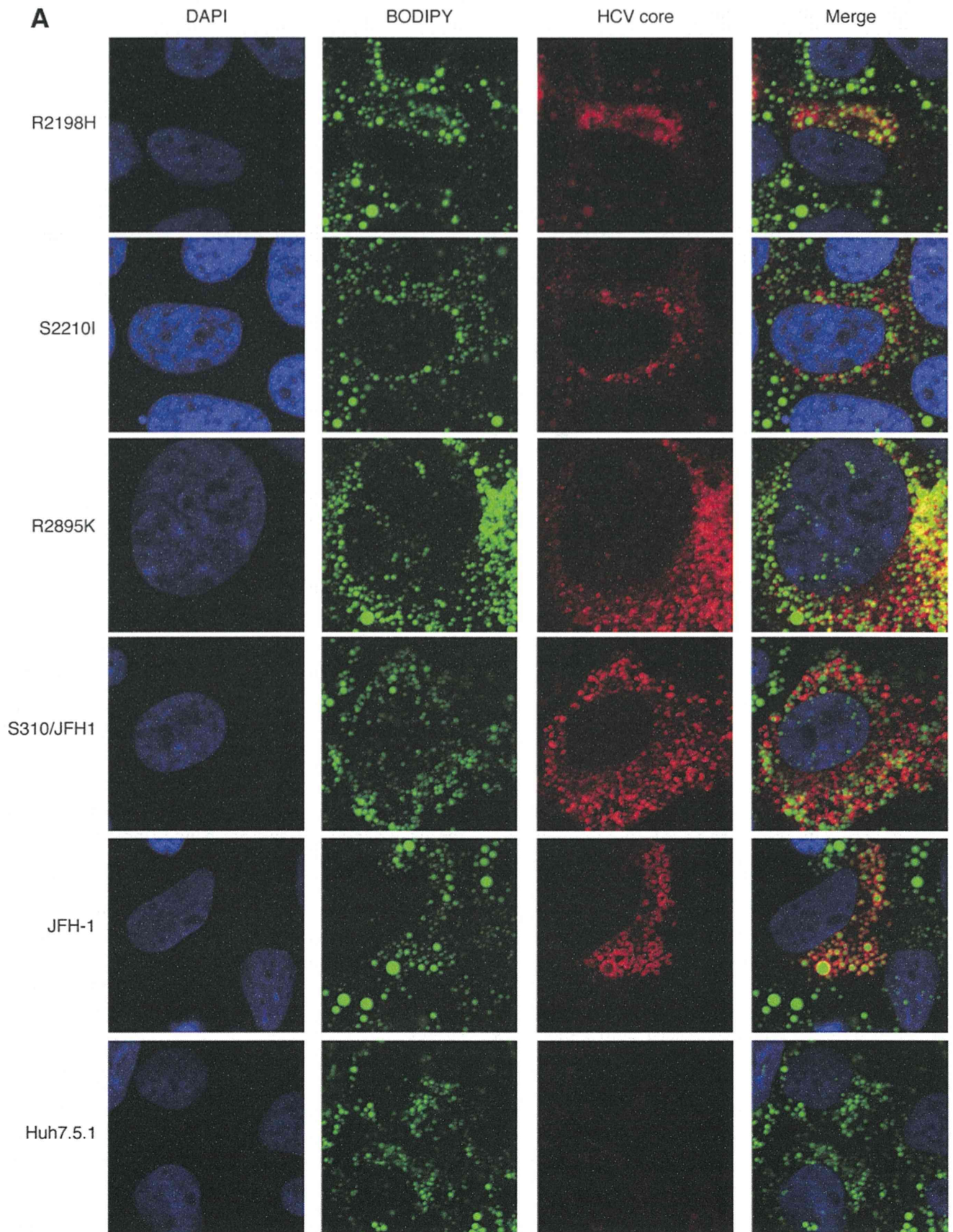
infection pathways as JFH-1 and J6/JFH1 chimeric virus, at least with respect to CD81.

To clarify the pathogenesis of genotype 3a infection, cellular sublocalization of HCV core protein and LDs in the S310-infected cells was performed with confocal microscopy. We synthesized RNA of three S310 clones (R2198H, S2210I, and R2895K), S310/JFH1 chimera, and JFH-1 and transfected the synthesized RNA into Huh7.5.1 cells. The cells were passaged every 3-5 days, and passaged cells were seeded onto a slide glass. We used BODIPY, a marker for LDs. S310-derived core proteins showed punctate patterns instead of ring-like patterns and were mainly found in the cytoplasm (Fig. 4A). S310-derived core proteins were not located around the LDs. By contrast, in the JFH-1 virus-infected cells, core proteins colocalized with LDs and exhibited ring-like patterns corresponding to the surfaces of LDs, as previously reported (Fig. 4A).<sup>27</sup> To confirm the intracellular localizations of HCV core protein and LDs, we magnified a partial area of each image and displayed the intensity of both fluorescences (Fig. 4B). We selected the representative region of interest (ROI1) and drew a line in each image. Inten-

sity profiles along the line are shown on the right of the images, and red and green lines indicate the fluorescence intensities of HCV core protein and LDs, respectively. Figure 4B demonstrates that S310-derived core proteins were localized in the cytoplasm and not around the LDs, whereas JFH-1-derived core proteins were colocalized around the surfaces of LDs. These results suggest that the virus particle production pathway may be different between S310 and JFH-1 viruses.

Next, we quantified the lipid content in the infected cells. JFH-1 wild-type virus, S310 viruses (S2210I, T2496I, and R2895K) and S310/JFH1 chimeric virus were inoculated into Huh7.5.1 cell cultures at an MOI of 0.2. Inoculated cells and Huh7.5.1 cells were passaged every 3-5 days. After 11 times of serial passages, core protein, LDs, and nuclei were visualized in the cells. Representative cell images are shown in Fig. 5A. Core proteins (red) were more strongly stained in S310 virus-infected cells, and no core protein staining was observed in Huh7.5.1 cells. The LD staining (green) in the virus-infected cells was higher than in

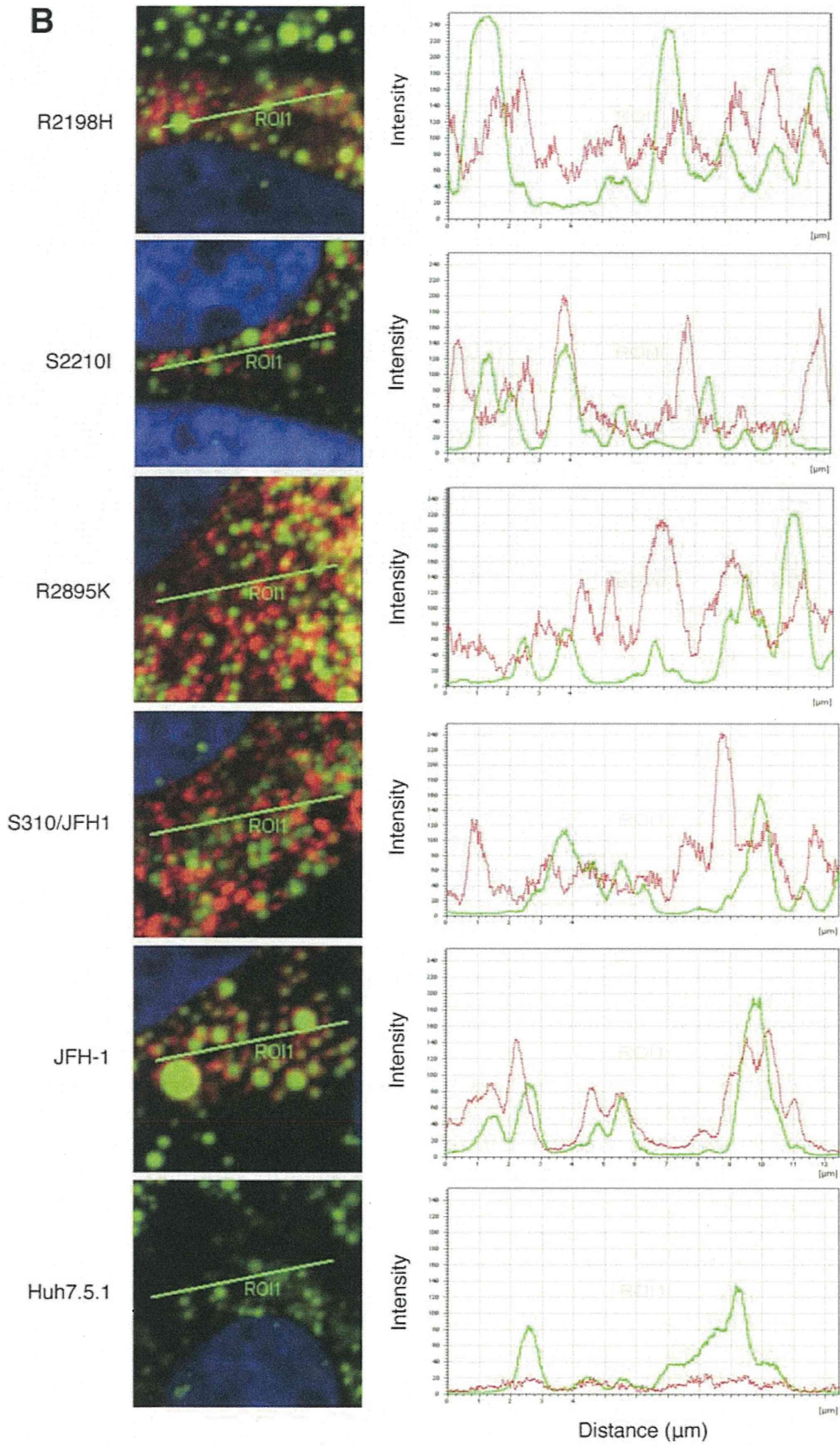
F5



C  
O  
L  
O  
R

Fig. 4. Localization of HCV core proteins and lipid droplets. (A) Huh7.5.1 cells were transfected with the transcribed RNA from each construct. The cells were passaged every 3-5 days, and passaged cells were seeded onto a slide glass. The cells were fixed, probed with the core-specific antibody (red), BODIPY for lipid droplets (green), and DAPI for nucleus staining (blue), and examined by confocal microscopy. Cells at 61 days after transfection are shown. (B) Each merged image was magnified and a line was drawn across the region of interest (ROI1). Intensity profiles along the line are shown on the right of the images. The red line indicates the fluorescence intensity of HCV core protein, and the green line indicates the fluorescence intensity of LDs. The y-axis indicates arbitrary units of fluorescence intensity.





C  
O  
L  
O  
R

Fig. 4. (Continued)

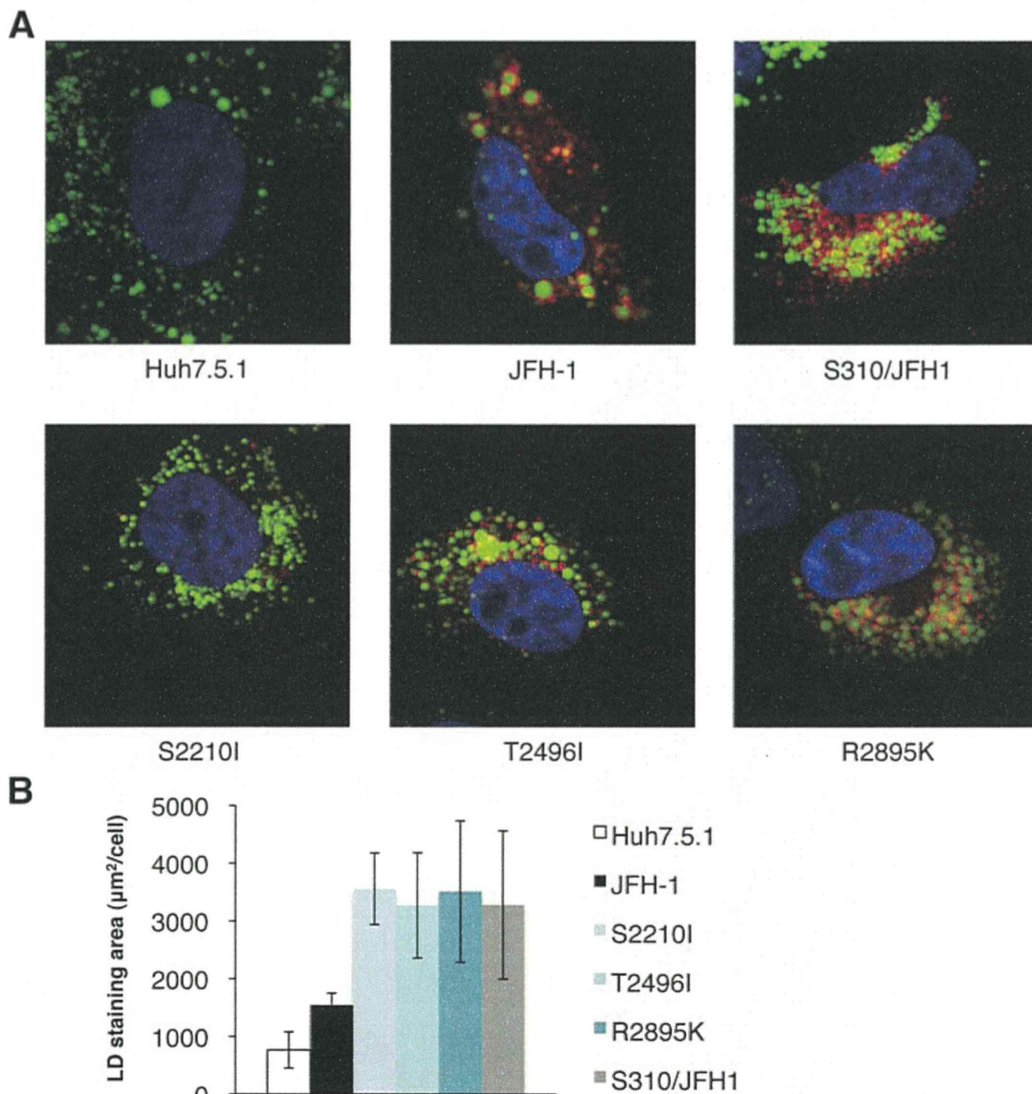


Fig. 5. Quantification of the LD content in cells. (A) Huh7.5.1 cells were inoculated with S310 viruses and JFH-1 wild-type virus at an MOI of 0.2. After 11 serial passages, the cells were analyzed as described in the Fig. 4A legend. (B) The mean values of the LD staining area in 7 cells (from Huh7.5.1 cells and JFH-1 infected cells) or 11 cells (from S310 and S310/JFH1 infected cells) were measured by MetaMorph analysis for each Huh7.5.1 cells and virus-infected cell. The y-axis indicates LD staining area. Mean values  $\pm$  standard deviations are shown.

Huh7.5.1 cells. Furthermore, the LD staining area in the S310 virus (S2210I, T2496I, and R2895K)- and S310/JFH1-infected cells was further greater than in JFH-1-infected cells (Fig. 5A). For the statistical analysis, we selected representative similar sized cells and measured the LD staining area in a single cell by MetaMorph analysis. We analyzed seven cell images each from Huh7.5.1 cells and JFH-1, and 11 cell images each from S310/JFH1 and S310 virus-infected cells. JFH-1 infected cells exhibited significantly higher LD staining levels than Huh7.5.1 cells ( $P < 0.0005$ ). S310 virus and S310/JFH1 chimeric virus-infected cells exhibited significantly much higher LD staining levels than Huh7.5.1 cells ( $P < 0.0001$ ) and than JFH-1 infected cells ( $P < 0.005$ ).

**Antiviral Drug Activities Against S310 Viruses.** We tested several antiviral drugs against S310 (genotype 3a) and JFH-1 (genotype 2a) infections. In the preliminary experiments, secreted HCV core protein levels were detected in parallel with intracellular HCV RNA levels. We thus used the secreted HCV core protein level as a marker of antiviral activity and determined IC<sub>50</sub> values against HCV replication (Table 3). Huh7.5.1 cells were inoculated with S310 and JFH-1 viruses at an MOI of 0.2 with or without NS3 protease inhibitor (VX-950), nucleoside polymerase inhibitor (PSI-6130), nonnucleoside polymerase inhibitor (JTK-109), NS5A inhibitor (BMS-790052), CsA, and IFN $\alpha$ . We selected the three S310 viruses (S2210I, T2496I, and R2895K) with NS3, NS5A, or

COLOR

T3

**Table 3. Antiviral Drug Activities Against HCV Infection**

	VX-950 (nM)	BMS-790052 (pM)	PSI-6130 ( $\mu$ M)	JTK-109 ( $\mu$ M)	CsA ( $\mu$ M)	IFN- $\alpha$ (IU/mL)
JFH-1	31.2 $\pm$ 18.7	20.0 $\pm$ 16.8	3.4 $\pm$ 1.7	8.7 $\pm$ 2.1	0.5 $\pm$ 0.2	0.1 $\pm$ 0.1
S2210I	9841.0 $\pm$ 1026.1	48.1 $\pm$ 59.1	1.4 $\pm$ 0.1	0.7 $\pm$ 0.1**	0.2 $\pm$ 0.1	4.2 $\pm$ 4.0
T2496I	436.6 $\pm$ 81.7*	24.4 $\pm$ 23.4	5.6 $\pm$ 5.2	2.3 $\pm$ 0.6**	0.7 $\pm$ 0.6	0.2 $\pm$ 0.2
R2895K	436.3 $\pm$ 249.8*	10.2 $\pm$ 1.7	1.6 $\pm$ 0.2	1.4 $\pm$ 1.2**	0.9 $\pm$ 0.8	4.6 $\pm$ 3.7

Assays were performed in triplicate and IC<sub>50</sub> values are expressed as mean  $\pm$  standard deviations.

\* $P < 0.05$  versus JFH-1.

NS5B adaptive mutations (Table 1). In VX-950 treatment, IC<sub>50</sub> values for S310 infection seemed to be higher than for JFH-1 infection; however, a statistically significant increase was only observed with T2496I virus infection as compared to JFH-1 virus infection (Table 3). This lack of significance may be due to the large experimental deviation in other S310 virus infections. PSI-6130 inhibited both genotype virus infections at similar levels. However, JTK-109 was significantly more effective against S310 viruses than JFH-1 virus ( $P < 0.05$ ). BMS-790052, CsA, and IFN $\alpha$  inhibited both JFH-1 and S310 viruses at similar levels. There were no differences in antiviral drug efficacies among S310 clones except for VX-950. Adaptive mutations in these three clones may not be important for drug efficacies. Cell viability was determined by the WST-1 assay, and there was no cellular toxicity within the tested dose of the drugs (data not shown).

## Discussion

In the present study we established a cell-culture-adapted genotype 3a infectious virus system. In a previous study, adaptive mutations were important for efficient replication of a genotype 3a subgenomic replicon (S310).<sup>9</sup> Therefore, we introduced these mutations into full-length S310 constructs to determine if these constructs can replicate and produce infectious virus particles in cell culture. Full-length S310 wild-type virus did not exhibit increased intracellular and extracellular core levels. However, some of the full-length S310 viruses with adaptive mutations displayed increased intracellular and extracellular core levels in a transient virus production assay (data not shown). To examine whether these clones could continuously produce infectious viral particles, we passaged the S310 RNA-transfected cells repeatedly and monitored the HCV core protein levels in the culture medium for 3 months. As a result, HCV core protein levels of the three clones with adaptive mutations (R2198H, S2210I, and R2895K) increased soon after the transfection and eventually plateaued. From 6 to 8 weeks after transfection, extracellular HCV core protein levels

of the other three clones with adaptive mutations (T2496I, R2895G, and T2496I + R2896K) increased rapidly, and their extracellular core protein levels also reached levels similar to the former three clones. All six clones showed sufficient viral RNA replication, virus production, and infectivity for autonomous virus expansion at the end of culture (D82). By sucrose density gradient analysis, we confirmed that S310 clones exhibited similar profiles of HCV core protein and RNA to JFH-1, but the peak infectivity titers were located in the same fraction as HCV core proteins and RNA. The peak infectivity of S310 clones shifted to the heavier fractions as compared to JFH-1. In a previous study, it was also reported that a particular mutant JFH-1 strain exhibited both HCV RNA and infectivity in the same fraction.<sup>28</sup> In that study, a point mutation (G451R) was identified in the viral E2 protein, and the G451R mutation was speculated to increase the density and infectivity of the virus particles.<sup>29</sup> It is thus possible that E2 proteins of S310 clones also alter the density of infectious viral particles. Upon inoculation of secreted S310 viruses into naïve Huh7.5.1 cells, both intracellular and extracellular core protein levels of infected cells were at levels similar to JFH-1 but less than J6/JFH1. In the neutralization experiment, S310 infections of Huh7.5.1 cells were sensitive to anti-CD81 and anti-E2 antibody treatment. Thus, these results suggest that S310 viruses can replicate efficiently and produce infectious virus particles.

Patients with genotype 3a HCV infections tend to develop hepatic steatosis, an intracellular accumulation of lipids and subsequent formation of LDs in the cytoplasm of hepatocytes.<sup>30</sup> S310-infected patient also showed microvesicular and macrovesicular steatosis both before and after liver transplantation. The LD is an organelle used for the storage of neutral lipids. Hepatic steatosis might be involved in inducing lipid synthesis by activation of SREBP-1 and peroxisome proliferator-activated receptor gamma (PPAR $\gamma$ ) or by producing reactive oxygen species.<sup>31-33</sup> Inversely, MTP and PPAR $\alpha$  might be involved in decreasing lipid secretion and degradation.<sup>34,35</sup>

In previous studies, cells expressing genotype 3a core protein were used to study the genotype 3a HCV core protein association with steatosis.<sup>11-13</sup> HCV genotype 3a core protein up-regulated the activity of fatty acid synthase promoter.<sup>36</sup> Domain 3 of the HCV core protein was sufficient for lipid accumulation, and specific polymorphisms in the HCV core protein of genotype 3a increased the lipid levels, contributing to steatosis in cultured cells.<sup>11</sup> However, the previous systems used only core protein expression, so they lacked the effects of other viral proteins and the entire viral life cycle. Furthermore, HCV core protein sublocalization on the LD surface is important for infectious virus particle formation.<sup>29</sup> We thus analyzed core protein and LD sublocalization by using the genotype 3a infection system. S310-derived core proteins showed punctate signals rather than the ring-like core protein staining pattern usually seen in JFH-1-infected cells (Fig. 4A). We further examined whether S310 infection resulted in the accumulation of LDs in a long-term culture of infected cells. Interestingly, S310 virus-infected cells exhibited greater LD accumulation than Huh7.5.1 cells and JFH-1 virus-infected cells. In addition, LD accumulation in the S310/JFH1 chimeric virus-infected cells was similar to S310 virus-infected cells. S310/JFH1 chimeric virus consists of the S310-derived structural region and the JFH-1-derived non-structural region. The result thus suggests that the S310-derived structural region is important for LD accumulation in the S310-infected cells. To examine the gene expression levels important for cellular lipid metabolism, we examined MTP, PPAR $\alpha$ , and SREBP-1c mRNA expression by real-time PCR. However, no differences in mRNA expression levels were found in between Huh7.5.1 cells and the infected cells (data not shown). Further detailed analysis will be necessary to clarify the mechanisms for LD accumulation in S310 virus-infected cells.

To provide new therapeutic approaches for genotype 3a HCV infections, we examined the antiviral drug activity against S310-infected cells. In VX-950 treatment, IC<sub>50</sub> values for S310 infection seemed to be higher than for JFH-1 infection; however, VX-950 was only statistically less effective for T2496I infection as compared to JFH-1 infection. In our previous study, another NS3 protease inhibitor, BILN-2061, was also less effective for the S310 subgenomic replicon as compared to the JFH-1 and Con1 replicons. JTK-109, a nonnucleoside polymerase inhibitor, was more effective for S310 than JFH-1. Other inhibitors, including NS5A inhibitor, nucleoside NS5B inhibitor, IFN $\alpha$ , and CsA, inhibited both viruses at similar levels. Thus,

this novel genotype 3a cell culture system can be used to assay possible antiviral compounds.

In conclusion, we established an HCV genotype 3a cell culture system. The patients infected with genotype 3a HCV appear to have different clinical characteristics than patients infected with other genotypes. This genotype 3a infectious cell culture system will be useful for studying the molecular mechanism of HCV viral life cycles and pathogenesis as well as for developing specific antiviral drugs for genotype 3a infections.

*Acknowledgment:* Huh7.5.1 cells were kindly provided by Dr. Francis V. Chisari. The J6CF plasmid was a kind gift from Dr. Jens Bukh. AP33 antibody was generously provided by Genentech. JTK-109 and PSI-6130 were generous gifts from Japan Tobacco, Inc., and Pharmasset, Inc., respectively.

## References

- Feld JJ, Liang TJ. Hepatitis C — identifying patients with progressive liver injury. *HEPATOLOGY* 2006;43:S194-206.
- Smith DB, Bukh J, Kuiken C, Muerhoff AS, Rice CM, Stapleton JT, et al. Expanded classification of hepatitis C Virus into 7 genotypes and 67 subtypes: updated criteria and assignment web resource. *HEPATOLOGY* 2014;59:318-327.
- Butt S, Idrees M, Akbar H, ur Rehman I, Awan Z, Afzal S, et al. The changing epidemiology pattern and frequency distribution of hepatitis C virus in Pakistan. *Infect Genet Evol* 2010;10:595-600.
- Rehman IU, Idrees M, Ali M, Ali L, Butt S, Hussain A, et al. Hepatitis C virus genotype 3a with phylogenetically distinct origin is circulating in Pakistan. *Genet Vaccines Ther* 2011;9:2.
- Hui JM, Kench J, Farrell GC, Lin R, Samarasinghe D, Liddle C, et al. Genotype-specific mechanisms for hepatic steatosis in chronic hepatitis C infection. *J Gastroenterol Hepatol* 2002;17:873-881.
- Rubbia-Brandt L, Quadri R, Abid K, Giostra E, Male PJ, Mentha G, et al. Hepatocyte steatosis is a cytopathic effect of hepatitis C virus genotype 3. *J Hepatol* 2000;33:106-115.
- Kumar D, Farrell GC, Fung C, George J. Hepatitis C virus genotype 3 is cytopathic to hepatocytes: reversal of hepatic steatosis after sustained therapeutic response. *HEPATOLOGY* 2002;36:1266-1272.
- Gottwein JM, Scheel TK, Jensen TB, Ghanem L, Bukh J. Differential efficacy of protease inhibitors against HCV genotypes 2a, 3a, 5a, and 6a NS3/4A protease recombinant viruses. *Gastroenterology* 2011;141:1067-1079.
- Saeed M, Gondeau C, Hmwe S, Yokokawa H, Date T, Suzuki T, et al. Replication of hepatitis C virus genotype 3a in cultured cells. *Gastroenterology* 2013;144:56-58 e57.
- Saeed M, Scheel TK, Gottwein JM, Marukian S, Dustin LB, Bukh J, et al. Efficient replication of genotype 3a and 4a hepatitis C virus replicons in human hepatoma cells. *Antimicrob Agents Chemother* 2012;56:5365-5373.
- Jhaveri R, McHutchison J, Patel K, Qiang G, Diehl AM. Specific polymorphisms in hepatitis C virus genotype 3 core protein associated with intracellular lipid accumulation. *J Infect Dis* 2008;197:283-291.
- Jhaveri R, Qiang G, Diehl AM. Domain 3 of hepatitis C virus core protein is sufficient for intracellular lipid accumulation. *J Infect Dis* 2009;200:1781-1788.
- Qiang G, Jhaveri R. Lipid droplet binding of hepatitis C virus core protein genotype 3. *ISRN Gastroenterol* 2012;2012:176728.
- Lindenbach BD, Evans MJ, Syder AJ, Wolk B, Tellinghuisen TL, Liu CC, et al. Complete replication of hepatitis C virus in cell culture. *Science* 2005;309:623-626.